The Link between Submillimeter and Radio Variability of Sgr A*
A Statistical Analysis of APEX and ATCA Data

M. Subroweit[1], M. García-Marín[1,2], A. Eckart[1,3], A. Borkar[1], M. Valencia-S.[1], G. Witzel[4], B. Shahzamanian[1], C. Straubmeier[1]

[1]I. Physikalisches Institut der Universität zu Köln (PH1), Zülpicher Straße 77, 50937 Köln, Germany [2]Space Telescope Science Institute, 3700 San Martin Drive, Baltimore, MD 21218, USA [3]Max-Planck-Institut für Radioastronomie (MPIfR), Auf dem Hügel 69, 53121 Bonn, Germany [4]Dep. of Physics and Astronomy, University of California Los Angeles (UCLA), 465 Portola Plaza, Los Angeles, CA 90095, USA

Introduction

The Milky Way hosts the supermassive black hole (SMBH) Sagittarius A* (Sgr A*) at its very center. Sgr A* constantly emits in the radio to submm domain with an emission maximum of ~ 3 Jy at about 350 GHz, the so called submm bump.
Additionally to the quiescent emission, short time scale ($\sim$ 1h) variability arising from the direct vicinity of Sgr A* has been observed across all bands. **The investigation of the flaring activity can provide important information about accretion and emission processes near to the SMBH**. Simultaneous multi-waveband observations have revealed a simultaneity of X-ray and IR flares and delayed flares from the submm to the radio domain. The link between IR/X-ray flares and delayed flares towards lower frequencies has successfully been modeled by adiabatically expanding synchrotron self-Compton components.
Analysis of multiwavelength campaigns have revealed that initial synchrotron turnover frequencies ν_0 are in the range of a few hundred GHz and expansion velocities $v_{\rm exp}$ may vary from 0.001 to 0.1 c. The NIR distribution is well described by a single state power-law process of the form $p(x) \propto x^{-\alpha}$ with a power-law index $\alpha \sim 4$. **In this work we investigate the short term variable flux density distributions at 345 and 100 GHz** and find that the variable sub-mm and radio emissions **are also power-law distributed with an index of about 4**. Our results put **additional constraints on flare emission models of Sgr A*** in general and to the adiabatically expanding plasmon model in particular.

The 345 GHz APEX Data

Between 2008 and 2014 8 APEX/LABOCA campaigns were carried out. With a beam size of 19″ the Galactic Center (GC) scans contain the extended sub-mm emission from the surroundings of the SMBH. To obtain light curves from Sgr A*, individual maps (Fig.1, left) are co-added and the resultant averaged central point source is subtracted. This procedure yields a model of the extended sub-mm emission from the GC (Fig.1, middle), which is subtracted from the individual scans. On the remaining flux density maps (Fig.1, right), Sgr A* is modeled as a point-source emitter. In this way 24 light curves with a total of 792 flux density values are obtained.
We extend the data set with additional literature data at comparable wavelengths (Fig.2). In total, the sub-mm data set contains 1137 values.

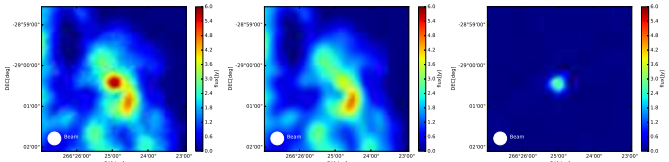

Figure 1: All maps show the innermost $3.5' \times 3.5'$ of the GC. Left: Single On-The-Fly scan from2 009-05-17T04:19:58. Middle: Model of the extended emission from the GC. Right: Remaining flux density map supposedly emitted from the vicinity of Sgr A*.

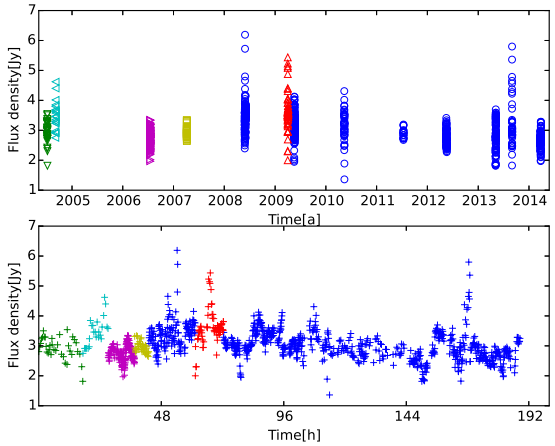

Figure 2: Top: All light curves between 2004 and 2014. The plot contains both APEX/LABOCA data (blue markers) and literature data (green: Eckart+09, SMA; cyan: Yusef-Zadeh+06, CSO; magenta: Yusef-Zadeh+08, CSO; yellow: Yusef-Zadeh+09, CSO; red: Trap+11, APEX). Bottom: A concatenated light curve, time gaps greater than 10 min were replaced by gaps of 300 s

The 100 GHz ATCA Data

Differential 100 GHz flux density light curves were collected with the Australia Telescope Compact Array (ATCA) for a total of 12 observation days during 2010 and 2014 (Fig.3, top). The used Compact Array Broadband Backend (CABB) has an average time resolution of 10 s. To make the time resolution similar to the LABOCA data, we average the differential flux values over 300 s. We obtain the positive high flux excursions by subtracting the lowest 10th percentile baseline from the data set and omitting all remaining non-physical negative flux density values (Fig.3, bottom).

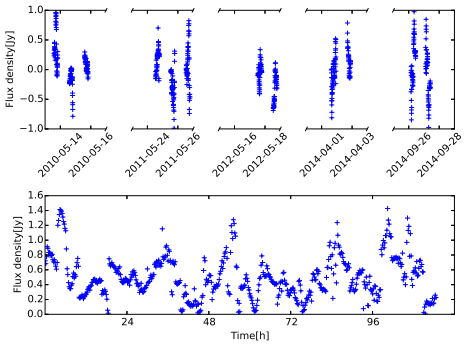

Figure 3: Top: All averaged differential 100 GHz light curves obtained with ATCA between 2010 and 2014. Bottom: A concatenated light curve of the averaged data after baseline subtraction and removal of negative fluxes. Time gaps greater than 10 min were replaced by gaps of 300 s.

Statistical Analysis

We investigate the flux density distributions for compatibility with a power-law distribution with a combined MLE/KS-statistics method (Rasc+09). We model the sub-mm emission with a shifted power-law of the form

$$p(x) \propto (x - s)^{-\alpha}. \quad (1)$$

The shift estimator s represents the contribution from the quiescent emission. For the analysis of the differential radio light curves we set $s = 0$.

Results

We find that both the **sub-mm and the radio emission is well described by a power-law distribution with an index of about 4** (sub-mm: $\alpha = 4.0 \pm 1.7$, radio: $\alpha = 4.7 \pm 0.8$). For the sub-mm distribution we also obtain an estimator for the quiescent emission $s = (2.8 \pm 0.6)$ Jy.

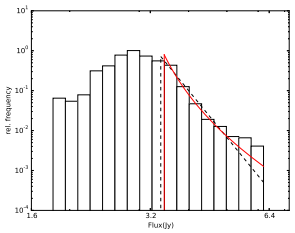

Figure 4: Histogram of the 345 GHz sub-mm emission. The distribution is well described by a shifted power-law (red) with a power-law index $\alpha \sim 4$.

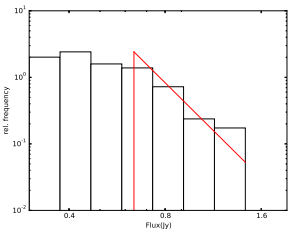

Figure 5: Histogram of the 100 GHz differential flux density values. The best fit power-law slope is also ~ 4

Consequences for the Adiabatic Expansion Model

The similarity of the power-law indices of both the 345 GHz and the 100 GHz distribution may put additional constraints on the model:

- **No significant contribution from source components with initial turnover frequencies at about 100 GHz.** If that would be the case, the 100 GHz flux density distribution contained not only power law distributed flux density values from expanded source components with $\nu_0 \sim 345$ GHz but also bright fluxes from components with $\nu_0 \sim 100$ GHz:

$$S(100\ \mathrm{GHz}, t) \sim S(\nu_0 \sim 100\ \mathrm{GHz}, t) + S_{\rm adiab}(\nu_0 \sim 345\ \mathrm{GHz}, t)\,. \quad (2)$$

  This would either lead to a power-law slope significantly below 4 or even destroy the power law characteristics in general.
- **No significant contribution from adiabatically expanding clouds with expansion velocities above 0.01 c.** The peak flux density $S_{\rm m}$ decrease due to adiabatic expansion can be written as

$$S_{\rm m} = S_{\rm m0} \left(\frac{R(t)}{R_0} \right)^{-(7p+3)/(p+4)} \quad (3)$$

  ($p \sim 2.5$: power-law index of the synchrotron energy spectrum, $R_0 \sim 1 R_{\rm S}$: initial blob size, $R(t)$: expanded blob size). With $1\mathrm{c} \equiv 100 R_{\rm S}\,\mathrm{h}^{-1}$ and typical delays of $t \sim 0.5$h between 345 and 100 GHz flares, expanding components with $v_{\rm exp} \gtrsim 0.01$c would lead to an excess of faint fluxes in the 100 GHz distribution. The power-law index then would be significantly above 4.

Conclusions

- Both the 345 Ghz and the 100 GHz variable flux density distribution can be described by a single state power-law process.
- The similarity of the power-law indices of the NIR, sub-mm and radio flare distribution ($\alpha \sim 4$) indicates same source components which strengthens the case for a plasmon/SSC model.
- Within the framework of the plasmon model, the similarity of the sub-mm and radio flare distribution narrows down possible initial turnover frequencies and expansion velocities to $\nu_0 > 100$GHz and $v_{\rm exp} < 0.01$c.